Spin polarization and giant magnetoresistance effect induced by magnetization in zigzag graphene nanoribbons

Ying-Tao Zhang*
College of Physics, Hebei Normal University, Shijiazhuang 050016, China

Hua Jiang and Qing-feng Sun
Beijing National Laboratory for Condensed Matter Physics and Institute of Physics, Chinese Academy of Sciences, Beijing 100190, China

X. C. Xie
Department of Physics, Oklahoma State University, Stillwater, Oklahoma 74078, USA
and Beijing National Laboratory for Condensed Matter Physics and Institute of Physics, Chinese Academy of Sciences, Beijing 100190, China

(Received 5 January 2010; revised manuscript received 3 March 2010; published 1 April 2010)

We investigate spin-dependent electron transport through a zigzag graphene nanoribbon sample with two ferromagnetic strips deposit on two sides of the graphene ribbon. Our results show that, for the antiparallel configurations of ferromagnetic strips, the conductance exhibits zero conductance plateau when the Fermi energy locates around the Dirac point and the sample shows the properties of a semiconductor. But for the parallel configurations, the energy band spectrum is metallic and the conductance is always equal to or larger than e^2/h. Thus the huge giant magnetoresistance effect can be achieved by altering the configurations of the ferromagnetic strips. Moreover, we study the spin-dependent conductance for the parallel configuration. It is found that the device shows half-metal behavior, in which it acts as a conductor to carriers of one spin orientation but as an insulator to those of the opposite spin orientation. So the present device can be applied as a spin filter. In addition, we study the consequence of the short-range Anderson disorder and find that the spin filtering effect and magnetoresistance effect still remain even in the strong disorder limit.

DOI: 10.1103/PhysRevB.81.165404 PACS number(s): 73.63.−b, 75.47.De, 73.20.−r, 85.35.−p

I. INTRODUCTION

Since the giant magnetoresistance (GMR) was discovered in 1988,[1,2] spintronics,[3,4] including spin transfer torque, semiconductor spintronics, molecular spintronics, and single-electron spintronics etc., which exploits the intrinsic spin of electrons, has been a new field of electronics. Especially, the hard disk technology based on the GMR of spin-valve structures has led to the fast rise in the density of stored information.[5,6] Recent development of GMR technology has also involved the tunneling magnetoresistance of the magnetic tunnel junctions, where the magnitude of the spin current depends on the magnetic orientation of the electrodes.[7]

Graphene, a single atomic layer of carbon with a planar hexagonal lattice, has attracted great attention[8,9] in both the physics and engineering communities due to its extraordinary electrical properties along with the discovery of mechanical cleavage of graphene from graphite crystals.[10,11] Various types of graphene based nanoelectronic devices have been fabricated and investigated, such as the graphene *p-n-p* junctions,[12,13] the *p-n* junctions,[14] the graphene-superconductor hybrid devices,[15] etc. At the same time, the development of graphene also opens a new and powerful way for the spintronic applications. Son *et al.*,[16] have demonstrated that graphene nanoribbons with zigzag edges can be made to carry a spin current in the presence of a sufficiently large electric field, which can therefore serve as the basis of the spintronic devices. From the first principles nonequilibrium transport method together with the density-functional theory, Kim *et al.*[17] have reported a large magnetoresistance in the spin-valve devices based on graphene nanoribbons. In particular, the experimental works exhibited that the spin coherence can extend over micrometer-scale distances in single graphene layers,[18] desirable for spin-based quantum computing and spintronics. Furthermore, Haugen *et al.*[19] have reported that ferromagnetic correlations can be induced by the so-called proximity effect in the graphene, which has recently been experimentally demonstrated.[20] Utilizing a graphene layer as the channel, the spin field effect transistor has also been proposed, where spin manipulation in graphene is achieved via electrical control of the electron exchange interaction with a ferromagnetic gate.[21] Recently, the spin injection into the graphene has been realized by several experimental groups,[22–26] using spin field effect transistor based on graphene.

The spin polarization and giant magnetoresistance are two important concepts in spintronics. Hwang *et al.*,[27] have predicted that the negative magnetoresistance can be achieved in intrinsic graphene and the nonmonotonic magnetoresistance can be produced in extrinsic graphene with a parallel magnetic field. The giant magnetoresistance is also predicted in a finite zigzag graphene nanoribbon bridging two metallic graphene electrodes.[28] Motivated by the above mentioned studies, we propose an alternative way to realize the spin polarization and giant magnetoresistance in the zigzag graphene nanoribbon. Our proposed system is a graphene nanoribbon in the (x,y) plane with the zigzag edge, as shown in Fig. 1, where two ferromagnetic stripes are deposited on

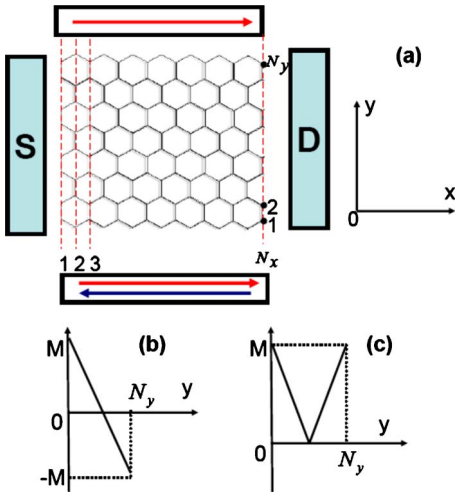

FIG. 1. (Color online) (a) Schematic of the device: two ferromagnetic stripes are placed on the top and bottom sides of the zigzag graphene nanoribbon and the source and drain leads are coupled to the graphene ribbon in the x direction. (b) and (c) are the magnetization distributions along the y direction in the graphene for the antiparallel (b) and parallel (c) configurations of two ferromagnetic stripes, where N_y is the number of atomic lattice sites in y direction, N_x is the number of vertical chains and M is the magnetization.

two sides of the graphene ribbon. The directions of the magnetization of the ferromagnetic stripes can be parallel or antiparallel, which can be tuned by a magnetic field. By applying the Landauer-Büttiker formalism combined with the nonequilibrium Green's function (NEGF) method, the spin-dependent current and conductance can be obtained. We find that a band gap is opened around the Dirac point for the antiparallel configuration, and the gap can reach the meV scale. But for the parallel configuration, there is no band gap. This indicates that a giant magnetoresistance can be produced when the Fermi energy E_F locates in the gap region. Furthermore, the current in the parallel configuration is completely spin-polarized in a large range of E_F around the Dirac point E_0. While $E_F > E_0$, the spin-polarized direction is same with the direction of the magnetic moment, but for $E_F < E_0$ it is in opposite direction with the magnetic moment. This means that the present device at the parallel configuration can work as a spin filter. In particular, the spin-polarized direction of this spin filter can be easily controlled by tuning the gate voltage. These results open a new possibility to generate spin-polarized current and giant magnetoresistance in the zigzag graphene nanoribbon.

The rest of the paper is organized as follows. In Sec. II we introduce the effective tight-binding model. The formulas and calculation method are also described. The numerical results and our discussions are presented in Sec. III. Finally, a conclusion is given in Sec. IV.

II. MODEL AND METHOD

With the tight-binding model, the Hamiltonian of π orbital electrons in the graphene is described by

$$H = \sum_{i,\sigma} (\varepsilon_i + \lambda_\sigma M_i) c_{i,\sigma}^\dagger c_{i,\sigma} + t \sum_{\langle i,j\rangle,\sigma} (c_{i,\sigma}^\dagger c_{j,\sigma} + \text{H.c.}), \quad (1)$$

where $c_{i,\sigma}^\dagger (c_{i,\sigma})$ creates (annihilates) an electron on site i with spin $\sigma(\sigma = \uparrow, \downarrow)$, $\lambda_\sigma = \pm 1$ for $(\sigma = \uparrow, \downarrow)$ and $\varepsilon_i = E_0 + w_i$ is the on-site energy. E_0 is the energy of the Dirac point, which is set zero as the energy zero point and w_i is the on-site disorder energy uniformly distributed in the range $[-W/2, W/2]$ with disorder strength W. $t(t \approx 2.75$ eV) is the nearest-neighbor hopping energy, which is chosen as the unit of energy in our calculations. Considering the two ferromagnetic strips attached on the two edges of the graphene ribbon, a magnetization M is induced in the graphene. Considering the experimental feasibility, the thin insulating layers can be deposited between graphene sample and ferromagnetic strips, which can block current leakage otherwise will occur. For the antiparallel configuration of ferromagnetic stripes, the magnetization decreases gradual from M to $-M$ along the y direction from one side to the other side of graphene [see Fig. 1(b)] But for parallel configuration, the magnetization is the biggest at the two sides ($y=1$ and $y=N_y$) with value M and gradually decreases to zero in the middle of graphene sheet [see Fig. 1(c)], because that the ferromagnetic stripes are attached on the two sides. Here we consider the linear decay of the magnetization from the edges to the center. But the results are similar for other types of decay models, e.g., the exponential decay. The distance of the nearest-neighbor carbon atoms $a = 0.142$ nm, which is also chosen as the unit of distance in our calculations.

For convenience, we assume that the ferromagnetic strips only act in the central region and the two clean and semi-infinite graphene leads are employed as source and drain leads and the temperature is set to zero. With the help of the NEGF method and the Landauer-Büttiker formula, the two-terminal spin-resolved conductance $G_{S(D)}^\sigma(E_F)$ is calculated from the formula[29]

$$G_{S(D)}^\sigma(E_F) = \frac{e^2}{h} Tr[\Gamma_S^\sigma(E_F) \mathbf{G}^{r,\sigma}(E_F) \Gamma_D^\sigma(E_F) \mathbf{G}^{a,\sigma}(E_F)], \quad (2)$$

where $\Gamma_{S(D)}^\sigma(E_F) = i\{\Sigma_{S(D)}^{r,\sigma}(E_F) - [\Sigma_{S(D)}^{r,\sigma}(E_F)]^+\}$ is the linewidth function. $\mathbf{G}^{r,\sigma}(E_F) = [\mathbf{G}^{a,\sigma}(E_F)]^+ = [E_F I - H_{cen} - \Sigma_S^{r,\sigma}(E) - \Sigma_D^{r,\sigma}(E)]^{-1}$ is the retarded Green's function with the Hamiltonian in the central region H_{cen}. $\Sigma_{S(D)}^{r,\sigma}(E_F)$ is the self-energy due to the semi-infinite source-(drain), which can be calculated numerically.[30]

III. NUMERICAL RESULTS

In the following numerical calculations, the width N_y is set to be $N_y = 52$ and the length N_x is set at $N_x = 400$. Corresponding to the current experimental situation, we limit the Fermi energy in the range of $E_F \leq 0.1t$ where the dispersion relation of graphene sheet is linear and exhibits the Dirac behavior. Let us start describing the transport property for the parallel and antiparallel configurations of ferromagnetic stripes in a clear graphene with the disorder strength $W = 0$. In Fig. 2, the conductance as function of Fermi energy for the alternative configurations of ferromagnetic stripes is studied. When the Fermi energy E_F locates around the Dirac

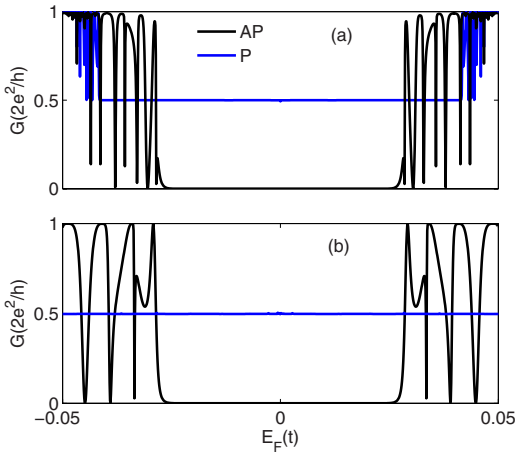

FIG. 2. (Color online) The conductance G as function of the Fermi energy E_F for the antiparallel (black line) and parallel (blue line) with the magnetization $M=0.05t$ (a) and $0.1t$ (b).

point, the conductance for the antiparallel configurations clearly shows zero conductance plateau. However, for the parallel configurations, the conductance exhibits the half-integer quantized plateau 1/2 in unit of $2e^2/h$. These behaviors indicate that the giant magnetoresistance can be achieved in the present device while E_F is set around the Dirac point. With increase in the magnetization M, range of the half-integer quantized conductance plateau for the parallel configurations is extended. But the range of the zero conductance for the antiparallel configuration is almost unchanged while M increases from $0.05t$ to $0.1t$. When E_F locates outside of the zero conductance or the half-integer plateaus, the conductances show strong oscillation for both parallel and antiparallel configurations, because of the mismatch of interfaces between the lead and the center conductor. The oscillation is between e^2/h and $2e^2/h$ for the parallel configuration, and between 0 and $2e^2/h$ for the antiparallel configuration.

In the above discussion, we only consider the GMR effect when N_y is even (zigzag configuration). In order to prove the robustness of the GMR effect in our scheme, we also calculate the conductance as a function of Fermi energy E_F for odd $N_y=53$ (shown in Fig. 3), corresponding to the so called "antizigzag" nanoribbons.[31,32] One can see that the conductance for the antiparallel configuration also shows the zero conductance plateau when the Fermi energy E_F locates around the Dirac point. For the parallel configuration, the conductance shows obvious oscillation in the whole E_F region with the amplitude ranging between $1.5e^2/h$ and $2e^2/h$, which is not same as the zigzag configuration (see Fig. 2). However these changes do not affect the robustness of the GMR effect in our scheme since the conductance in the parallel configuration is always larger than e^2/h in the entire energy region where there is zero conductance for the antiparallel one. So the GMR effect is still there. On the other hand, we should mention that the GMR effect is not apparent for the armchair graphene nanoribbon regardless of the width of nanoribbon.

In order to understand the zero conductance plateau for antiparallel configuration of ferromagnetic stripes and the giant magnetoresistance effect, we calculate the band structure of graphene nanoribbon with antiparallel and parallel configurations. Here we consider an infinite graphene nanoribbon with the periodic boundary condition in x direction and open boundary condition in y direction.[33] From the band structure (in Fig. 4), one can see that the energy band gap opens up near the Dirac point for the antiparallel configuration, leading to a zero conductance when the Fermi energy located in the band gap. But for parallel configuration of ferromagnetic strips, the band structure shows no energy gap for magnetization in the range from $-3t$ to $3t$. So the conductance is always finite. These results also illuminate that the graphene ribbon with antiparallel configuration of ferromagnetic strips shows the semiconductor property, while the metallic property is remained for the parallel configuration. Thus, the magnetoresistance is very large in the present graphene ribbon device.

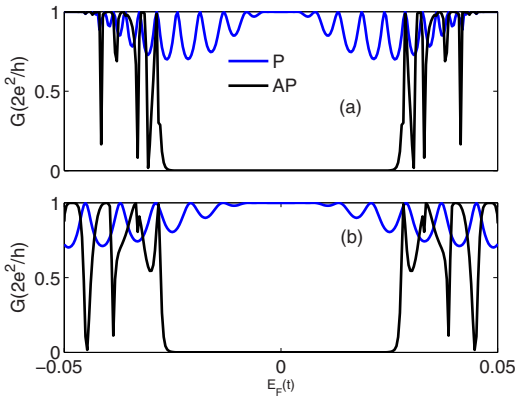

FIG. 3. (Color online) The conductance G as function of the Fermi energy E_F for the antiparallel (black line) and parallel (blue line) with the magnetization $M=0.05t$ (a) and $0.1t$ (b), corresponding to the "antizigzag" nanoribbons.

In the above calculations, we take the magnetization $M=0.05t$ and $0.1t$. In a real experimental condition, M may

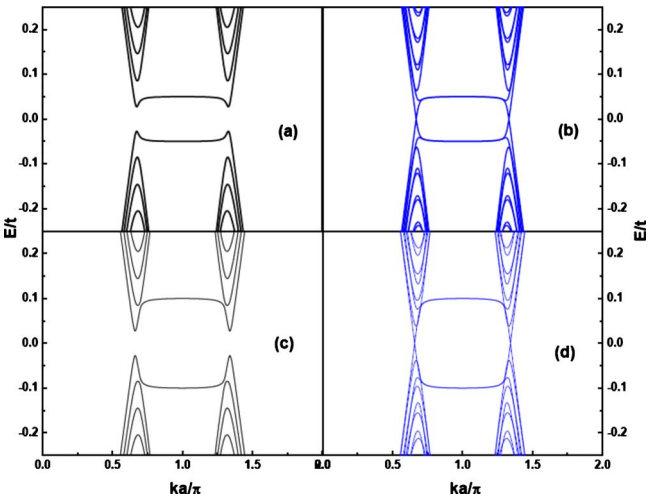

FIG. 4. (Color online) The energy band structures for the antiparallel configuration (a and c) and parallel configuration (b and d). The width $N_y=52$ and the magnetization $M=0.05t$ in the panels (a) and (b) and $0.1t$ in the panels (c) and (d).

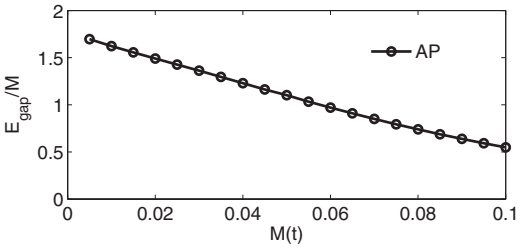

FIG. 5. The ratio of the energy gap to the magnetization M as a function of M.

be quite small. For instance, by growing the graphene on a ferromagnetic insulator (e.g., EuO), its magnetization M is only about 5 meV,[19] thus, about $0.002t$. However, the results obtained in this paper still hold for smaller M. In Fig. 5, the ratio of the energy gap E_{gap} for the antiparallel configuration to magnetization M as a function of M is plotted. When the Fermi energy E_F is within the energy gap E_{gap}, the conductance is zero for the antiparallel configuration and is $\geq e^2/h$ for the parallel configuration, so the device has a large magnetoresistance. From Fig. 5, it is obvious that the ratio of E_{gap}/M increases monotonically with decrease in the magnetization and the ratio E_{gap}/M exceeds 1 when M is small. In other words, the energy gap E_{gap} exists and its value is larger than the magnetization M in a real experimental situation. Taking $M=0.002t$, for example, the energy gap $E_{gap} \approx 1.5M$ is larger than the energy k_BT for temperature $T=70$ K.

As shown in Fig. 2, the presence of the half-integer quantized conductance plateau for the parallel configuration of ferromagnetic stripes actually indicates half-metallicity, in which one spin channel opens completely but the other spin channel is closed. In order to understand this result, we present the spin-dependent conductance for the parallel configuration in Fig. 6. For $M=0t$ [see Fig. 6(a)], the conductances of the spin-up and spin-down electrons are completely equal since the system is a clean zigzag graphene sheet.[34] As M is set to be nonzero, the conductance of the spin-up channel remains at the quantized conductance plateau when the

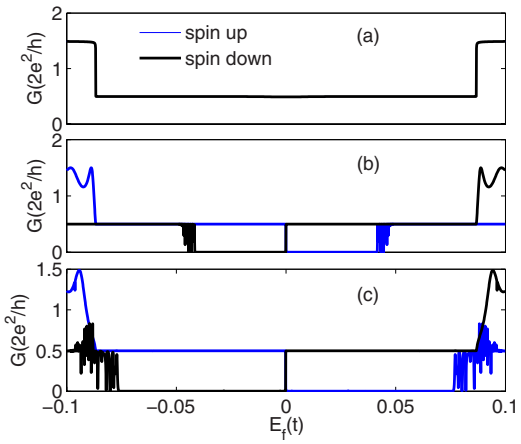

FIG. 6. (Color online) Spin-dependent conductance G as a function of the Fermi energy E_F for the parallel magnetization $M=0t$ (a), $M=0.05t$ (b), and $M=0.1t$ (c).

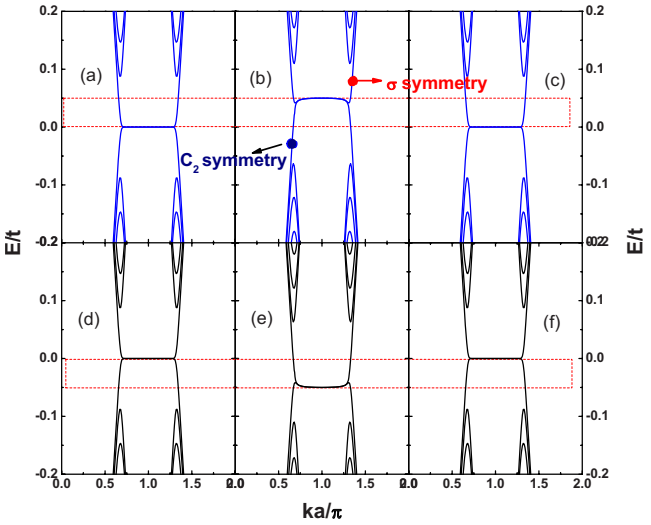

FIG. 7. (Color online) The energy band structures of the source lead (a) (d), central region (b) (e), and drain lead (c) (f) for the parallel magnetization $M=0.05t$. The panels (a), (b), and (c) stand for the spin-up electrons while the panels (d), (e), and (f) are for the spin-down electrons.

Fermi energy E_F is below zero, but an abrupt breakdown from the quantized conductance plateau to zero conductance plateau occurs when the Fermi energy E_F passes zero (i.e., at the Dirac point). But for the spin-down channel, it shows the opposite behavior. The conductance is at zero plateau while $E_F<0$, abruptly jumps to e^2/h at the Dirac point, and keeps at the half-integer plateau for $E_F>0$. Moreover, comparing Figs. 6(b) and 6(c), the ranges of the zero and the half-integer conductance plateaus for spin-up or spin-down channels are extended with increase in the magnetization M (e.g., from $0.05t$ to $0.1t$).

To get a better understanding of the spin-dependent conductance behavior in the parallel configuration of ferromagnetic strips, in Fig. 7, we plot the spin-dependent band structures of the source lead, the central region, and the drain lead. It was found that for a region around the band center, the energy bands above and below the Dirac point show opposite orbital symmetry [see Fig. 7(b)]. The upper energy bands with respect to the Dirac point show σ symmetry in which the wave functions exhibit the even parity. In contrast, the lower energy bands have C_2 symmetry in which the wave functions exhibit the odd parity.[17] As shown in Fig. 6(b), the magnetization lifts up the energy bands for the spin-up electrons in the central region and causes the orbital symmetry difference between the two leads and the central region for the energy region in the red dash frame in Figs. 7(a)–7(c). On the other hand, in the same energy region, the spin-down electrons exhibit the same orbital symmetry for these three regions. Due to the parity conservation of the transverse wave functions and the band-selection rule,[35] only electrons having the same parity as the wave functions of the central region can pass through. Thus, only the spin-down electrons can take part in the transport process when the Fermi energy is above zero, and the zigzag graphene ribbon is an insulator for the spin-up electrons in this case. But the situation is exactly opposite when E_F is below zero. In this case

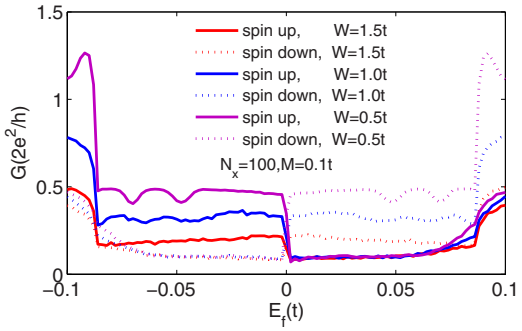

FIG. 8. (Color online) Spin-dependent conductance G as a function of the Fermi energy E_F for different disorder strengths W. The parameters are $M=0.1t$ and $N_x=100$.

($E_F<0$), the spin-up electrons have the same orbital parity in the two leads and the central region, so they can transport through the device, while the conductance for the spin-down channel is zero now. Due to the nature of half-metal that acts as a conductor to carriers of one spin orientation but as an insulator to those of the opposite orientation, the graphene nanoribbon can be used as a novel spin filter device, desirable for spintronic application. Here we want to stress that the spin is completely polarized and the spin-polarization orientation can be controlled by electric means in the present spin filter device. By tuning the gate voltage, the Fermi energy E_F can be controlled. While $E_F>0$, the spin-polarized direction of the current is in the spin-down direction, but for $E_F<0$ it is in the spin-up direction.

Finally, we consider the effect of the short-range Anderson disorder on the spin-polarized current and the large magnetoresistance. The results exhibit that they are stable against the disorder. Figure 8 presents the effect of disorder on the spin-dependent conductance, where the conductance is averaged over up to 1000 random disorder configurations. In the presence of a disorder potential, the transverse wave functions in the central region are no longer odd or even functions of the transverse position y. Thus the fraction of spin-down (up) electrons also takes part in the transport process when the Fermi energy is lower (higher) than zero. This means the current of the minor spin component is not zero and the spin polarization is not complete. But the conductance for the minor spin component still is small, and in our simulation it is about $0.2e^2/h$ and remains in this value for a broad range of disorder strength W (from $0.5t$ to $1.5t$). On the other hand, the conductance for the major spin component (i.e., the spin-up electrons at $E_F<0$ or the spin-down electrons at $E_F>0$) is also slightly affected by the weak disorder (for $W=0.5t$). With increase in the disorder strength, the major spin-component conductance becomes smaller and smaller, but it maintains a plateau structure. Even for $W=1.5t$, the lowest conductance plateau is well established with its plateau value at $0.4e^2/h$. Notice that this value $0.4e^2/h$ is still twice larger than the minor spin-component conductance. This indicates that the current is still well spin polarized even for the disorder strength around $1.5t$. Thus the high and stable spin-polarized current can be produced based on the present graphene nanoribbon device.

IV. CONCLUSIONS

In summary, we present spin polarization and giant magnetoresistance effect in zigzag graphene nanoribbon modulated by configurations of ferromagnetic strips. For the antiparallel configuration, an energy band gap is opened by the magnetization. So the conductance is zero when the Fermi energy locates inside the gap (i.e., around the Dirac point), and the graphene nanoribbon shows the properties of a semiconductor in this situation. But for the parallel configuration, the energy band spectrum remains gapless as in a clean graphene, and the conductance is $\geq e^2/h$. Thus the huge giant magnetoresistance can be achieved in this graphene device. Furthermore, we study the spin dependent conductance and energy band spectrum for the parallel configuration of ferromagnetic strips. The graphene nanoribbon shows half-metallicity since it acts as conductor to electrons of one spin orientation but as an insulator to those of the opposite orientation. So the device can be applied as a spin filter and its current is completely spin polarized. In addition, we find that the spin-polarization direction in present spin filter current can be conveniently controlled by the electric scheme, i.e., by only tuning the gate voltage. Finally, we study the effect of disorder on the spin-polarization current and magnetoresistance. The results show that the disorder slightly weakens the spin polarization, but the spin filtering effect and magnetoresistance effect are well maintained even with strong disorder.

ACKNOWLEDGMENTS

We gratefully acknowledge the financial support from NSF-China under Grants No. 10647126 and No. 10974236, the 973 Program Project No. 2009CB929103, and Natural Science Foundation of Hebei Province of China under Grant No. A2010000339. X.C.X. is supported by U.S.-DOE (Grant No. DE-FG-02-04ER46124) and Oklahoma C-Spin center.

*zhangyt@mail.hebtu.edu.cn

[1] M. N. Baibich, J. M. Broto, A. Fert, F. Nguyen Van Dau, F. Petroff, P. Etienne, G. Creuzet, A. Friederich, and J. Chazelas, Phys. Rev. Lett. **61**, 2472 (1988).

[2] G. Binasch, P. Grünberg, F. Saurenbach, and W. Zinn, Phys. Rev. B **39**, 4828 (1989).

[3] I. Zutic, J. Fabian, and S. D. Sarma, Rev. Mod. Phys. **76**, 323 (2004).

[4] A. Fert, Rev. Mod. Phys. **80**, 1517 (2008).

[5] S. S. P. Parkin, in *Spin Dependent Transport in Magnetic Nanostructures*, edited by S. Maekawa and T. Shinjo (Taylor & Francis, London, 2002), p. 237.

[6] C. Chappert, A. Fert, and F. Nguyen Van Dau, Nature Mater. **6**, 813 (2007).

[7] J. S. Moodera, L. R. Kinder, T. M. Wong, and R. Meservey, Phys. Rev. Lett. **74**, 3273 (1995).
[8] A. H. Castro Neto, F. Guinea, N. M. R. Peres, K. S. Novoselov, and A. K. Geim, Rev. Mod. Phys. **81**, 109 (2009) and references therein.
[9] C. W. J. Beenakker, Rev. Mod. Phys. **80**, 1337 (2008).
[10] K. S. Novoselov, A. K. Geim, S. V. Morozov, D. Jiang, Y. Zhang, S. V. Dubonos, I. V. Grigorieva, and A. A. Firsov, Science **306**, 666 (2004).
[11] K. S. Novoselov, A. K. Geim, S. V. Morozov, D. Jiang, M. I. Katsnelson, I. V. Grigorieva, S. V. Dubonos, and A. A. Firsov, Nature (London) **438**, 197 (2005).
[12] B. Huard, J. A. Sulpizio, N. Stander, K. Todd, B. Yang, and D. Goldhaber-Gordon, Phys. Rev. Lett. **98**, 236803 (2007).
[13] B. Özyilmaz, P. Jarillo-Herrero, D. Efetov, D. A. Abanin, L. S. Levitov, and P. Kim, Phys. Rev. Lett. **99**, 166804 (2007).
[14] W. Long, Q. F. Sun, and J. Wang, Phys. Rev. Lett. **101**, 166806 (2008); J. Li and S.-Q. Shen, Phys. Rev. B **78**, 205308 (2008).
[15] Q. Zhang, D. Fu, B. Wang, R. Zhang, and D. Y. Xing, Phys. Rev. Lett. **101**, 047005 (2008); Q. Liang, Y. Yu, Q. Wang, and J. Dong, *ibid.* **101**, 187002 (2008); S.-G. Cheng, Y. Xing, J. Wang, and Q.-F. Sun, *ibid.* **103**, 167003 (2009); Q.-F. Sun and X. C. Xie, J. Phys.: Condens. Matter **21**, 344204 (2009).
[16] Y.-W. Son, M. L. Cohen, and S. G. Louie, Nature (London) **444**, 347 (2006).
[17] W. Y. Kim and K. S. Kim, Nat. Nanotechnol. **3**, 408 (2008).
[18] N. Tombros, C. Jozsa, M. Popinciuc, H. T. Jonkman, and B. J. van Wees, Nature (London) **448**, 571 (2007).
[19] H. Haugen, D. Huertas-Hernando, and A. Brataas, Phys. Rev. B **77**, 115406 (2008).
[20] C. Józsa, M. Popinciuc, N. Tombros, H. T. Jonkman, and B. J. van Wees, Phys. Rev. Lett. **100**, 236603 (2008).
[21] Y. G. Semenov, K. W. Kim, and J. M. Zavada, Appl. Phys. Lett. **91**, 153105 (2007).
[22] E. W. Hill, A. K. Geim, K. Novoselov, F. Schedin, and P. Blake, IEEE Trans. Magn. **42**, 2694 (2006).
[23] S. Cho, Y. F. Chen, and M. S. Fuhrer, Appl. Phys. Lett. **91**, 123105 (2007).
[24] W. H. Wang, K. Pi, Y. Li, Y. F. Chiang, P. Wei, J. Shi, and R. K. Kawakami, Phys. Rev. B **77**, 020402(R) (2008).
[25] H. Goto, A. Kanda, T. Sato, S. Tanaka, Y. Ootuka, S. Odaka, H. Miyazaki, K. Tsukagoshi, and Y. Aoyagi, Appl. Phys. Lett. **92**, 212110 (2008).
[26] C. Józsa, M. Popinciuc, N. Tombros, H. T. Jonkman, and B. J. van Wees, Phys. Rev. B **79**, 081402(R) (2009).
[27] E. H. Hwang and S. Das Sarma, Phys. Rev. B **80**, 075417 (2009).
[28] F. Muñoz-Rojas, J. Fernández-Rossier, and J. J. Palacios, Phys. Rev. Lett. **102**, 136810 (2009); J.-C. Chen, S.-G. Cheng, S.-Q. Shen, and Q.-F. Sun, J. Phys.: Condens. Matter **22**, 035301 (2010).
[29] S. Datta, *Electronic Transport in Mesoscopic Systems* (Cambridge University Press, Cambridge, England, 1995); S. Datta, *Quantum Transport: Atom to Transistor* (Cambridge University Press, Cambridge, England, 2005).
[30] D. H. Lee and J. D. Joannopoulos, Phys. Rev. B **23**, 4997 (1981); M. P. Lopez Sancho, J. M. Lopez Sancho, and J. Rubio, J. Phys. F: Met. Phys. **14**, 1205 (1984); **15**, 851 (1985).
[31] A. R. Akhmerov, J. H. Bardarson, A. Rycerz, and C. W. J. Beenakker, Phys. Rev. B **77**, 205416 (2008).
[32] A. Cresti, G. Grosso, and G. P. Parravicini, Phys. Rev. B **77**, 233402 (2008).
[33] Y. Hatsugai, Phys. Rev. B **48**, 11851 (1993).
[34] N. M. R. Peres, A. H. Castro Neto, and F. Guinea, Phys. Rev. B **73**, 195411 (2006).
[35] J. Nakabayashi, D. Yamamoto, and S. Kurihara, Phys. Rev. Lett. **102**, 066803 (2009).